

## Biologically Formed Mesoporous Amorphous Silica

Martin Jensen,<sup>†</sup> Ralf Keding,<sup>†</sup> Thomas Höche,<sup>‡</sup> and Yuanzheng Yue<sup>\*,†</sup>

Section of Chemistry, Aalborg University, DK-9000 Aalborg, Denmark, and Leibniz Institute for Surface Modification, Permoserstraße 15, D-04318 Leipzig, Germany

Received November 21, 2008; E-mail: yy@bio.aau.dk

**Abstract:** Mesoporous crystalline silica has attracted the attention of scientists due to its extraordinary functionalities. In particular, substantial progress has been made in the synthesis of mesoporous crystalline silica using biomimetic approaches under ambient conditions. However, the biomimetic synthesis of mesoporous amorphous silica has not been well studied so far. Here we show that amorphous silica can be synthesized in aqueous solution under ambient conditions via biological catalysis. The high purity amorphous silica is obtained as spicules (average diameter: 15.6  $\mu\text{m}$ ) that are cemented through junctions, thereby forming the skeleton of the freshwater sponge *Cauxi*. We discover that such amorphous spicules themselves contain mesopores. This opens a potential avenue to develop highly durable mesoporous membranes at room temperature. We also describe the macro- and microstructural features, the mechanism of biological precipitation, and the properties of the *Cauxi* skeleton.

### Introduction

Due to its outstanding properties, amorphous silica (or silica glass) is used in a wide variety of applications, e.g., membranes,<sup>1</sup> columns,<sup>2</sup> heat-proof materials,<sup>3</sup> optical communication fibers,<sup>4</sup> and catalysts in organic synthesis.<sup>5</sup> Amorphous silica with high purity<sup>6–9</sup> and/or with specific structure<sup>8,10,11</sup> can be obtained using different synthesis approaches such as fusing,<sup>6,7</sup> sol–gel,<sup>8,10</sup> and argon plasma methods.<sup>7</sup> In the past few years, mesoporous silica has drawn much attention due to its extraordinary functionalities.<sup>12–14</sup> Actually it has become possible to synthesize the mesoporous crystalline silica via biomimetic approaches under ambient conditions.<sup>15,16</sup> However, to our best knowledge, the biomimetic synthesis of mesoporous amorphous silica has not been reported. Recently, it was recognized that the freshwater sponge *Cauxi* (in some cases, called *Cauxi* or Porifera, Demospongiae) found in the Amazon basin consists of amorphous needle-like silica that has been used for fiber-reinforcing pottery by the precolumbian natives.<sup>17</sup> Further investigation of the structural features of such biologically synthesized materials is expected to elucidate the composition and the texture down to the mesoscale. This is mandatory for developing an understanding of the bioprecipitation process taking place in *Cauxi*. In this paper, we report the detailed characterization of the *Cauxi* skeleton and provide insights into the mechanisms of its biological synthesis. The findings of this study will be crucial

in the development of biomimetic approaches for the synthesis of mesoporous, amorphous silica with high purity under ambient condition.

### Experimental Section

**Extraction of the Sponge.** The freshwater sponge *Cauxi* was collected at the river bank of the Rio Negro at Praia Grande in the Amazon basin 60 km west of Manaus, Brazil (3°03'22.5S and 60°30'33.56W).

**Bleaching.** A selected amount of the sponge was added to a Teflon container and mixed with 35% H<sub>2</sub>O<sub>2</sub>, 69% HNO<sub>3</sub>, and water in the volume ratio 8:7:1. The Teflon container was placed in a 90 °C water bath for 20 min to accelerate the removal of organic material from the sponge. The solvents were then removed and fresh solvents added. The container was replaced in the water bath for 20 min. The procedure was repeated until a white material without any colorants remained in the container. The solvents were then removed, and the material was rinsed once with water. The material was heated at 160 °C for 2 h to vaporize any remaining bleaching agents and, at the same time, to keep the bulk properties of the sponge skeleton unchanged.

- (6) Bruckner, R. J. *Non-Cryst. Solids* **1970**, *5*, 123–174.
- (7) Tohmon, R.; Shimogaichi, Y.; Mizuno, H.; Ohki, Y.; Nagasawa, K.; Hama, Y. *Phys. Rev. Lett.* **1989**, *62*, 1388–1391.
- (8) Monnier, A.; Schüth, F.; Huo, Q.; Kumar, D.; Margolese, D.; Maxwell, R. S.; Stucky, G. D.; Krishnamurty, M.; Petroff, P.; Firouzi, A.; Janicke, M.; Chmelka, B. F. *Science* **1993**, *261*, 1299–1303.
- (9) Angell, C. A. *Science* **1995**, *267*, 1924–1935.
- (10) Zhao, D. Y.; Feng, J. L.; Huo, Q. S.; Melosh, N.; Fredrickson, G. H.; Chmelka, B. F.; Stucky, G. D. *Science* **1998**, *279*, 548–552.
- (11) Kresge, C. T.; Leonowicz, M. E.; Roth, W. J.; Vartuli, J. C.; Beck, J. S. *Nature* **1992**, *359*, 710–712.
- (12) Asefa, T.; Yoshina-Ishii, C.; MacLachlan, M. J.; Ozin, G. A. *J. Mater. Chem.* **2000**, *10*, 1751–1755.
- (13) Sathe, T. R.; Agrawal, A.; Nie, S. *Anal. Chem.* **2006**, *78*, 5627–5632.
- (14) Stein, A. *Adv. Mater.* **2003**, *15*, 763–775.
- (15) Cha, J.; Stucky, G. D.; Morse, D. E.; Deming, T. J. *Nature* **2000**, *403*, 289–292.
- (16) Che, S.; Liu, Z.; Ohsuna, T.; Sakamoto, K.; Terasaki, O.; Tsumu, T. *Nature* **2004**, *429*, 281–284.
- (17) Costa, M. L.; Kern, D. C.; Pinto, A. H. E.; Souza, J. R. T. *Acta Amazonica* **2004**, *34*, 165–178.

<sup>†</sup> Aalborg University.

<sup>‡</sup> Leibniz Institute for Surface Modification.

- (1) de Vos, R. M.; Verweij, H. *Science* **1998**, *279*, 1710–1711.
- (2) Dai, J.; Yang, X.; Carr, P. W. *J. Chromatogr., A* **2003**, *1005*, 63–82.
- (3) Saito, K.; Ogawa, N.; Ikushima, A. J.; Tsurita, Y.; Yamahara, K. *J. Non-Cryst. Solids* **2000**, *270*, 60–65.
- (4) Tong, L. M.; Gattass, R. R.; Ashcom, J. B.; He, S. L.; Lou, J. G.; Shen, M.; Maxwell, I.; Mazur, E. *Nature* **2003**, *426*, 816–819.
- (5) Minakata, S.; Kano, D.; Oderaotshi, Y.; Komatsu, M. *Angew. Chem., Int. Ed.* **2004**, *43*, 79–81.

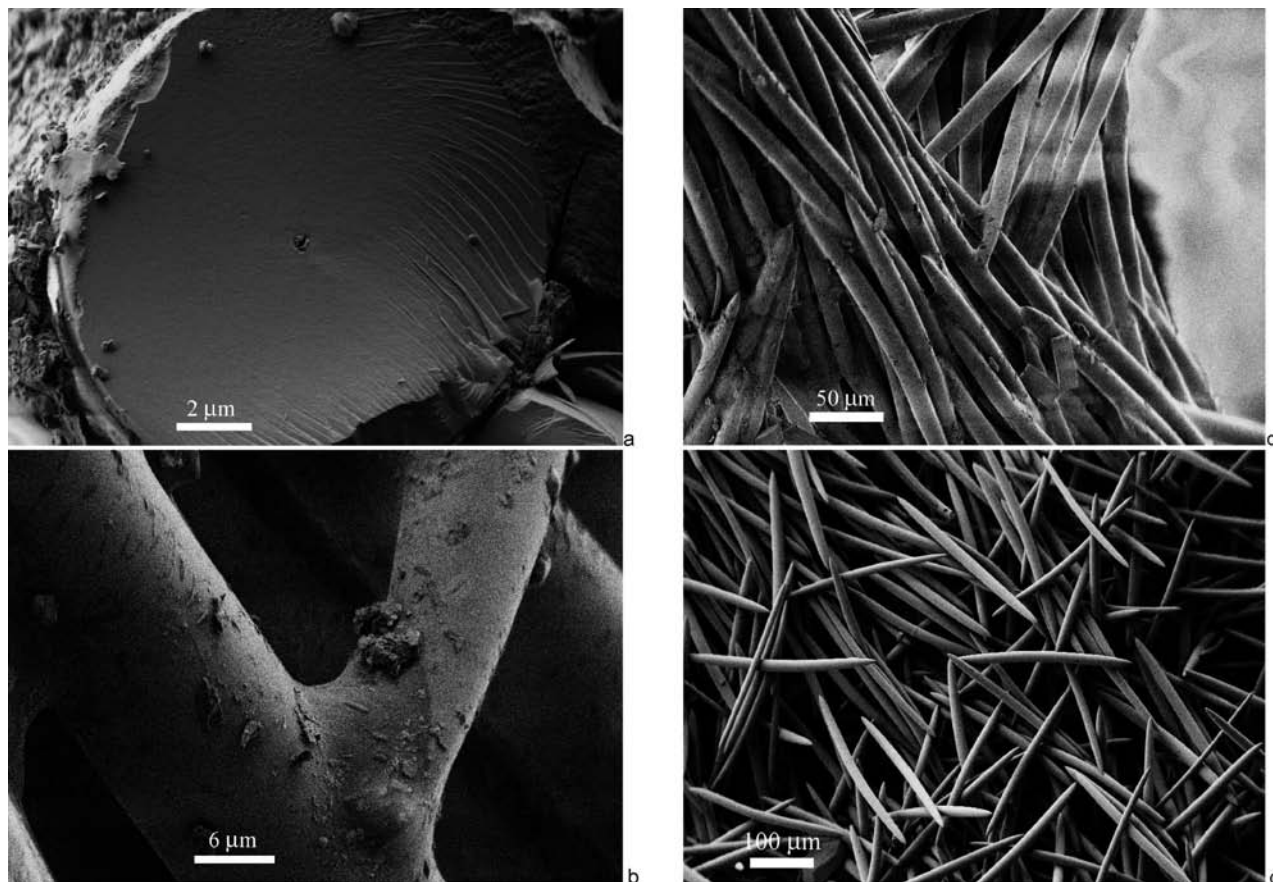


**Figure 1.** Secondary-electron micrographs of the spicules constituting the skeleton of *Cauxi*. (a) Cross-section crack of spicule showing the axial channel, the solid structure, and material on the surface. (b) Junction cementing the spicules. (c) The spicules of the sponge arranged in a bundled structure. (d) Bleached sponge showing the destruction of the bundled structure by the removal of organic material and coating.

**Thermal Analysis.** A simultaneous thermal analyzer (STA) (NETZSCH STA 449C Jupiter (Selb, Germany)) was used to obtain both the differential scanning calorimetric (DSC) signals and the mass change of the samples. During the thermal analysis, a platinum crucible containing the sample and an empty reference platinum crucible were placed on the sample carrier at room temperature. Initially both crucibles were held 5 min at an initial temperature of 333 K. Thereafter, an upscan to 1543 K and a subsequent downscan were performed at 10 K/min. The samples underwent a second up- and downscan with 10 K/min to determine the standard glass transition temperature ( $T_g$ ).<sup>18</sup> The purge gas for the thermal analysis was air with a flow of 40 mL/min. Before measuring each sample, a baseline was measured by using two empty crucibles according to the above-stated heating procedure and then used for correcting the DSC signal of the samples. The isobaric heat capacity ( $C_p$ ) as a function of temperature was obtained by comparing the DSC signals of a reference sample (sapphire) with those of the sponge. From the STA measurements, the mass change of the sample was obtained as a function of temperature.

**Heat Treatments.** A sponge sample was put in a porcelain crucible and heat-treated in a muffle furnace (Scandiaovnen A/S, Denmark) in air at 823 K for 7 h. This heat treatment condition was selected to ensure complete removal of all organic substances. Another sample was prepared by heating untreated sponge in an alumina crucible in air to 1723 K for 17 h in an electric furnace (Ängelholm, Sweden) to crystallize the material.

**SEM and TEM Imaging.** Scanning electron microscopy (SEM) of uncoated samples was done using a Zeiss 1540 XB scanning electron microscope (Oberkochen, Germany), using secondary

electrons for imaging. The untreated sponge annealed at 1723 K for 17 h was finely ground using an agate mortar. The obtained powder was thoroughly dispersed in isopropanol, and subsequently a droplet of the dispersion was dried on a carbon-coated copper grid. The ground, heat-treated sponge fragments on the grid were imaged using high-resolution transmission electron microscopy (TEM) (JEOL JEM 4010, acceleration voltage 400 keV, point-to-point resolution: 0.155 nm).

**X-ray Fluorescence.** Approximately 2 g of bleached sponge powder was mixed with 24 g of  $\text{Li}_2\text{B}_4\text{O}_7$ . The mixture was melted at approximately 1573 K and made into a tablet. X-ray fluorescence (XRF) measurement was performed after calibration using a S4-Pioneer X-ray spectrometer (Bruker-AXS, Karlsruhe, Germany).

**Vacuum Hot Extraction.** The water content of the bleached fibers was measured by mass spectrometry coupled with vacuum hot extraction.<sup>19</sup> Prior to measurement, the sample was kept at 473 K for 2 h to remove adsorbed water and cooled to room temperature within the device. Subsequently, the degassing rate was recorded when heating the sample at a rate of 10 K/min to 1773 K.

**Optical Microscopy.** The length and width of the spicules were measured using a Zeiss Axioskop microscope. The length of the fibers was measured employing a 10 $\times$  lens. The width was

(18) Yue, Y. Z. *J. Non-Cryst. Solids* **2008**, *354*, 1112–1118.

(19) Mueller, R.; Gottschling, P.; Gaber, M. *Glass Sci. Technol.* **2005**, *78*, 76–89.

(20) Shimizu, K.; Cha, J.; Stucky, G. D.; Morse, D. E. *Proc. Natl. Acad. Sci. U.S.A.* **1998**, *95*, 6234–6238.

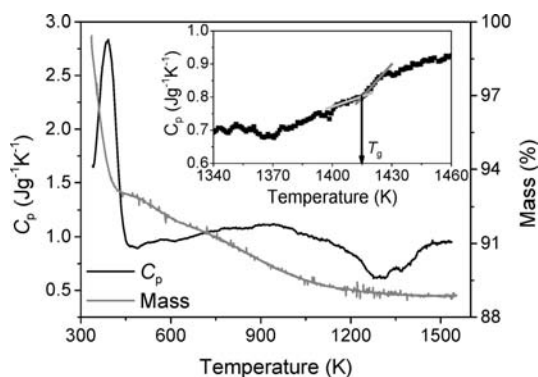


**Figure 2.** DSC and TG upscan in air on the bleached sponge. The DSC upscan reveals an initial endothermic peak until around 450 K where the TG curve demonstrates a mass loss. Another endothermic peak occurs in the DSC patterns around 1400 K. Inset: DSC upscan in the range 1300–1500 K. The gray lines in the inset are used to determine  $T_g$ .

measured as the broadest point of the fiber with a  $100\times$  lens. Both width and length were measured for 50 fibers.

## Results and Discussion

The sponge skeleton consists of spicules that are made of glassy silica with an organic coating. Similar to other sponges, an axial filament is present in the spicule (Figure 1a).<sup>20–22</sup> The spicules of *Cauxi* are cemented by junctions (Figure 1b) to form bundles (Figure 1c) composing the *Cauxi* skeleton. To determine the chemical composition and the thermochemical properties of the inorganic part of the sponge, it was bleached with  $\text{HNO}_3$  and  $\text{H}_2\text{O}_2$ . The bleaching process destroys the bundled structure and removes the organic material from the surface of the spicules, while the spicule structure itself remains unaffected (Figure 1d). The organic material present in the untreated sponge was combusted by heat treatment as well, and this destroys the bundled structure. The resulting product of the bleaching process was white powder, whereas that of the combustion was orange powder. The junctions are organic, since they were decomposed by both chemical and thermal treatments. The tempered spicules possess residual mineral surface layers that consist predominantly of iron oxides causing the orange color observed after heat treatment. Due to the solubility of the inorganic surface species in acid, the bleached sample comprises uncoated silica spicules. In other types of sponges reported in literature, silica cemented spicules with a coaxial structure gain mechanical flexibility by a hierarchical arrangement.<sup>23</sup> The organic binder leads to a superior mechanical stability of *Cauxi* compared to sponges with coaxial spicules, as the latter cannot sustain shear or bending, but only impedes crack propagation.

The composition of the bleached sponge was examined using the vacuum hot extraction (VHE) method up to 1780 K for volatile components and by XRF for the remaining inorganic components. Water is the dominant volatile constituent (5.5 wt% of bleached spicules). After removal of water, the inorganic part consists of  $\sim 99.7$  wt%  $\text{SiO}_2$  and traces of  $\text{CaO}$  and  $\text{Al}_2\text{O}_3$ . The next question is whether the 5.5 wt% water are incorporated into the amorphous silica network structure or resides in pores

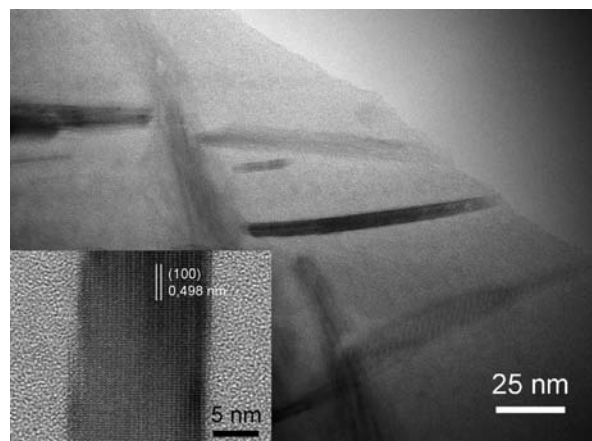


**Figure 3.** Bright-field transmission electron micrograph of a spicule after the heat treatment at 1723 K for 17 h. Inset: Close-up high-resolution transmission electron micrograph of a single channel after crystallization.

or spheres in the spicules? To clarify this, characterizations of the bleached samples were performed using DSC, TEM, and small-angle X-ray scattering (SAXS). Figure 2 shows the DSC upscan curve of the bleached sponge in air at a heating rate of 10 K/min. There is an endothermic peak at  $\sim 450$  K, which is attributed to initial vaporization of superficial water. This is verified by a mass loss in the same temperature region (see the gray curve in Figure 2). In addition, a broad weak endothermic response is observed at  $\sim 1400$  K which is a typical feature of the glass transition of the glassy silica. The DSC pattern of untreated sponge is similar to that of the bleached one except for an exothermic peak between 500 and 900 K due to combustion of organic material. The inset in Figure 2 shows the endotherm at  $\sim 1400$  K, where an increase in the heat capacity is clearly seen. This endotherm must be associated with the glass transition of silica.<sup>24</sup> This suggests that the *Cauxi* skeleton is amorphous and this is also confirmed by XRD as reported elsewhere.<sup>17</sup> By applying a previously suggested method,<sup>18</sup> the  $T_g$  of the spicules of the bleached sponge was found to be  $\sim 1414$  K. As is known, the  $T_g$  of silica is rather sensitive to the hydroxyl groups incorporated in the glass network structure.<sup>25,26</sup> To estimate the water content in the network structure of the *Cauxi* spicules, it is necessary to know the relationship between the  $T_g$  and the hydroxyl content. To establish this relationship, the  $T_g$  of commercial silica glasses with 1, 150, and 1000 ppm water was measured and found to be 1438, 1425, and 1375 K, respectively. From the  $T_g$ –hydroxyl content relationship, it can be concluded that the spicules of *Cauxi* contain 400 ppm hydroxyl species, i.e., structural water. This value strongly differs from the water content of 5.5 wt% measured using VHE, indicating that the majority of the 5.5 wt% water does not belong to the glass network but, instead, exists as a separate phase. The existence of water in a separate phase is in contrast to other sponges.<sup>27</sup> Besides hydroxy groups, impurities such as  $\text{CaO}$  and  $\text{Al}_2\text{O}_3$  can also reduce the  $T_g$  of the silica glass.<sup>28</sup> The traces of  $\text{CaO}$  and  $\text{Al}_2\text{O}_3$  in the powder must reside outside the spicules rather than within the glass structure.

(21) Cha, J. N.; Shimizu, K.; Zhou, Y.; Christiansen, S. C.; Chmelka, B. F.; Stucky, G. D.; Morse, D. E. *Proc. Natl. Acad. Sci. U.S.A.* **1999**, *96*, 361–365.  
 (22) Aizenberg, J.; Sundar, V. C.; Yablon, A. D.; Weaver, J. C.; Chen, G. *Proc. Natl. Acad. Sci. U.S.A.* **2004**, *101*, 3358–3363.  
 (23) Aizenberg, J.; Weaver, J. C.; Thanawala, M. S.; Sundar, V. C.; Morse, D. E.; Fratzl, P. *Science* **2005**, *309*, 275–278.

(24) Richet, P.; Bottinga, Y.; Denielou, L.; Petitet, J. P.; Tequi, C. *Geochim. Cosmo. Acta* **1982**, *46*, 2639–2658.  
 (25) Deubener, J.; Müller, R.; Behrens, H.; Heide, G. *J. Non-Cryst. Solids* **2003**, *330*, 268–273.  
 (26) Mysen, B. O.; Richet, P. *Silicate Glasses and Melts*; Elsevier: Amsterdam, 2005.  
 (27) Sanford, F. *Microsc. Res. Tech.* **2003**, *62*, 336–355.

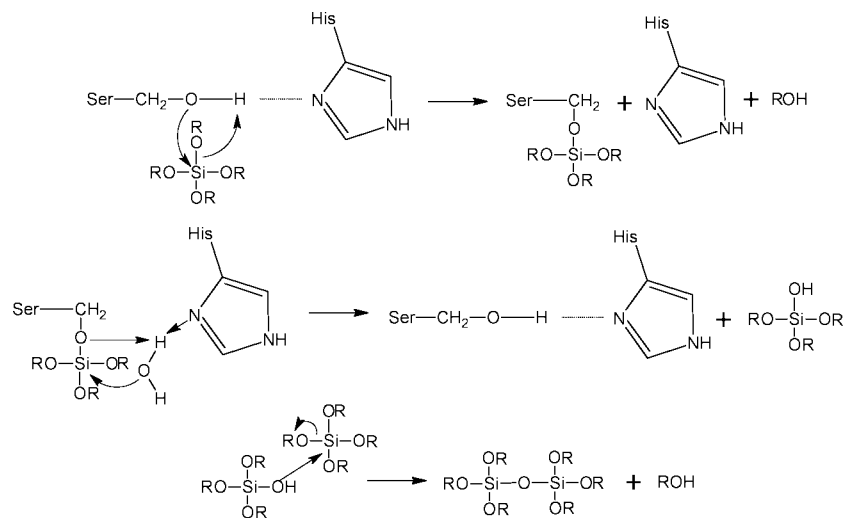


**Figure 4.** The silicate in  $\alpha$  catalyzed polymerization mechanism of silica as suggested in ref 21. Ser and His do not denote the entire serine and histidine residue, respectively, but only the remaining part of the residue. Dashed lines represent hydrogen bonds. A nucleophilic attack on the silicon atom displaces an alcohol and forms a covalent siloxane bond. Upon hydrolysis, a free hydroxyl group is created on the silicon. Finally, the hydrolyzed silicon species reacts with another silicon species under displacement of alcohol.

This is because their presence in glass structure would dramatically reduce  $T_g$ , which was not observed here. Figure 2 proves the  $T_g$  of the sponge to be rather similar to that of commercial silica glasses.<sup>28</sup> The  $T_g$  of the purified sponge skeleton is  $\sim 60$  K lower than that of pure silica glass reported in the literature.<sup>29</sup> Therefore, the lower  $T_g$  in the *Cauxi* spicules is predominantly due to the presence of hydroxyl groups in the glass structure.

Since the majority of water vaporizes between 700 and 1100 K during the VHE experiment (cf. Supporting Information), the water must reside inside some sort of mesosized channels. To verify this, both TEM and SAXS measurements were conducted. Due to pronounced decomposition, TEM images of untreated spicules could not be obtained. Although the bleached sample underwent massive radiation damage upon TEM inspection, the amorphous nature of the spicules was doubtlessly disclosed. TEM images of sponge fragments heat-treated at 1723 K for 17 h in air, however, reveal mesoscale crystalline phases embedded in the amorphous phase. As shown in Figure 3, crystalline phases possess a width of 10 to 15 nm and a length of up to 200 nm. This implies that the heat treatment at 1723 K first lead to removal of the water from some type of mesopores (Figure 2, TG curve) and second to the crystallization of amorphous layers on the surfaces of the mesopores. Thus, we can infer that the *Cauxi* skeleton indeed contains mesopores. Due to surface nucleation effects, the crystallization occurs more easily at the wall of mesopores than at other places in the bulk part of the spicules. From XRD measurements, the main crystalline phase is cristobalite (see Supporting Information), and high-resolution TEM micrographs also confirm the formation of cristobalite channels (Figure 3). From the inset of Figure 3 it is clearly seen that the crystalline channel is embedded in the amorphous matrix. The inset further shows that the growth direction relative to the wall of the mesopores is along [100]. SAXS confirms the presence of channels in the untreated sponge with a width and length of 23 and 110 nm, respectively (Supporting Information). In addition, a polymer structure with

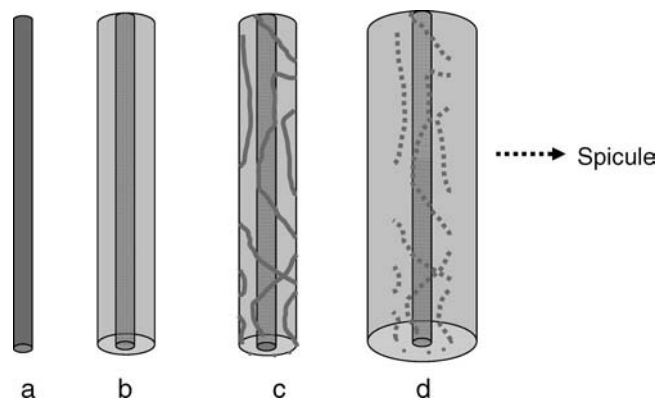


**Figure 5.** Schematic illustration of the growth mechanism of amorphous silica. (a) The sponge shoots a filament in the location, where it needs a new spicule for its skeleton structure. (b) The catalytic protein of the filament enables silica ( $\text{SiO}_2$ ) to grow until the active centers of the catalytic proteins are blocked by the formed silica layer. (c) The sponge deposits catalytic active protein strings on the outer surface of the growing silica rod. (d) Silica grows until the proteins are blocked by the further formed silica layer. The strings and the subsequent growth of silica lead to the mesosized channels. The process repeats until the final diameter of a spicule is reached.

a radius of gyration of 3.45 nm is detected (Supporting Information).

Like other siliceous sponges, *Cauxi* contains an axial filament known to harbor the silica catalyst protein known as silicatein  $\alpha$ .<sup>21</sup> The catalyzing mechanism of silicatein  $\alpha$  has previously been suggested as shown in Figure 4. Based on the characterization of *Cauxi*, we suggest the following growth mechanism (Figure 5). The sponge shoots the axial protein filament in the desired growth direction to attach to another spicule. This causes a slightly bent shape of the spicules (Figure 1d). Subsequently, silicatein  $\alpha$  polymerizes a thin silica layer around the filament. However, this silica deposition impedes transport of the siliceous acid to the axial filament, and a new set of protein strings containing silicatein  $\alpha$  are shot onto the newly synthesized silica deposition. This shooting process continues until the final diameter of spicules is reached. The polymer structures observed by SAXS are believed to be the protein strings residing in the

(28) Nascimento, M. L. F.; Zanotto, E. D. *Phys. Chem. Glasses: Eur. J. Glass Sci. Technol. B* **2007**, *48*, 201.

(29) Richet, P.; Bottinga, Y. *Geochim. Cosmochim. Acta* **1984**, *48*, 453–470.

mesopores. The axial filament is larger than the protein strings, as it contains macromolecules to provide mechanical stability in the river. Silicatein  $\alpha$  is capable of polymerizing silica, while it excludes the other elements found in the river water.

Besides the catalytic effect of the proteins, a driving force must be present to cause the glassy silica deposition. The pH value was 5.2 near the location where *Cauxi* was collected.<sup>30</sup> The pH value was  $\sim 4.5$  at 400–600 km further upstream in the Rio Negro,<sup>30</sup> where *Cauxi* cannot be found. The increase in pH diminishes the solubility of silica<sup>31</sup> enabling a supersaturation of the river with silica. Due to an activation energy of 76.6 kJ/mol for silica formation,<sup>32</sup> silica will not polymerize spontaneously, but a catalyst like the proteins found in the sponges is required to make silica synthesis possible.

The length and width of the *Cauxi* spicules were determined by optical microscopy to be  $305 \pm 18$  and  $15.6 \pm 1.5 \mu\text{m}$ , respectively. The narrow size distribution indicates rapid growth of the spicules, as found in other sponges.<sup>33</sup> A previous study demonstrated silicatein  $\alpha$  expressed in *E. coli* has a high capability of polymerizing silica *in vitro*.<sup>21</sup> Due to both findings, the synthesis approach via proteins could be of industrial relevance for synthesizing amorphous silica. In addition, this approach is of economic and technological interest, since the raw material ( $\text{SiO}_2$ ) is very abundant in nature and the synthesis requires only ambient conditions. This opens a new direction for the synthesis of the high value-added product amorphous,

mesoporous silica. Such silica can be potentially used as membranes for inverse osmosis, since it can sustain thermal cleaning of the membranes due to its thermal stability. Even the sponge-provided spicules could be used as a bioinert adsorbant host for proteins and larger molecules. Thereby, the gap between zeolites and conventional porous materials is filled in terms of application. The high temperature resistant spicules can also be utilized for manufacturing fiber-reinforced ceramics. However, further research still needs to be carried out to fully understand the actual biological formation process of the mesoporous amorphous silica. When such an understanding is achieved, a biomimetic mass production of the mesoporous amorphous silica will be possible.

In summary, the freshwater sponge *Cauxi* consists of an organic binder and a skeleton of amorphous, mesoporous silica of high purity. The catalyzing effect of the proteins enables the polymerization of this type of silica *in vitro*. Thus, a novel biomimetic approach for producing pure, mesoporous, amorphous silica under ambient conditions has been discovered.

**Acknowledgment.** We thank Morten Smedskjaer for helpful discussions. We also thank Ralf Müller, Jens Rafaelsen, Michael Zellmann, Jan Skov Petersen, and Christina Apfel for characterizations. T.H. gratefully acknowledges access to TEM facilities at MPI for Microstructure Physics in Halle, Germany, granted by U.M. Goesele.

**Supporting Information Available:** Additional experimental details. This material is available free of charge via the Internet at <http://pubs.acs.org>.

JA808847Y

(30) Küchler, I. L.; Miekeley, N.; Forsberg, B. R. *J. Braz. Chem. Soc.* **2000**, *11*, 286–292.

(31) Iler, R. K. *The Chemistry of Silica*; John Wiley: New York, 1979.

(32) Hurd, C. B.; Marotta, A. J. *J. Phys. Chem.* **1940**, *62*, 2767–2770.

(33) Imsiecke, G.; Steffen, R.; Custodio, M.; Borojevic, R.; Müller, W. E. G. *In Vitro Cell. Dev. Biol.* **1995**, *31*, 528–535.